

# Modeling the effect of freshwater inflows on the development of spring blooms in an estuarine embayment

Do-Seong Byun<sup>a,b,\*</sup>, Xiao Hua Wang<sup>a</sup>, Deirdre E. Hart<sup>c</sup>, Yang-Ki Cho<sup>b</sup>

<sup>a</sup> School of Physical Environmental and Mathematical Sciences, University of New South Wales at Australian Defence Force Academy, Canberra, ACT 2600, Australia

<sup>b</sup> Faculty of Earth Systems and Environmental Sciences/Institute of Marine Science, Chonnam National University, Gwangju 500-757, Republic of Korea

<sup>c</sup> Department of Geography, University of Canterbury, Private Bag 4800, Christchurch, New Zealand

Received 8 November 2004; accepted 2 June 2005

Available online 10 August 2005

## Abstract

Low vertical mixing rates are a key physical condition associated with the development of phytoplankton spring blooms in coastal and ocean waters. Vertical mixing rates in shallow coastal regimes are decreased not only by thermal stratification but also by haline stratification due to river runoff.

In this paper, the main physical processes involved in the onset of phytoplankton spring blooms are examined in a tide-dominated estuarine embayment, characterized by weak current velocities, using a 1-D ecosystem model (the European Regional Seas Ecosystem Model) coupled with a 3-D physical model (the Princeton Ocean Model coupled with a sediment transport model) via the off-line method. Simulation results show that a reduction in vertical mixing, caused by the episodic input of buoyant, freshwater inflows from a reservoir during the period of neap tides, is the main physical controlling process on the occurrence of spring algal blooms. Furthermore, sensitivity tests using: (1) layered and (2) depth-averaged monthly vertical eddy diffusivity values reveal that the timing of phytoplankton spring blooms in the model is strongly affected by the parameterization of vertical diffusivity.

© 2005 Elsevier Ltd. All rights reserved.

*Keywords:* spring blooms; haline stratification; freshwater discharge; vertical mixing; sea-surface cooling; Korea

## 1. Introduction

Marine phytoplankton bloom dynamics between winter and spring are significantly affected by the reduction in vertical mixing rates caused by changes in light availability (Cloern, 1991; Townsend et al., 1992). In general, an increase in solar radiation due to seasonal changes in the solar elevation leads to a reduction in

vertical mixing and thermal stratification in the water column in the mid to high latitudes.

Since the early work of Gran and Braarud (1935), the relationship between “mixing depth” and “critical depth” has commonly been used as an indicator for the onset of phytoplankton spring blooms (e.g., Sverdrup, 1953; Smetacek and Passow, 1990; Nelson and Smith, 1991). The original concept of “critical depth” is defined by Gran and Braarud (1935) as the depth at which the gross primary production in the water column is equal to the total respiration by the plankton.

Sverdrup (1953) pioneered the quantification (parameterization) of critical depth as a function of light intensity alone, based on several assumptions, including

\* Corresponding author. Faculty of Earth Systems and Environmental Sciences/Institute of Marine Science, Chonnam National University, Gwangju 500-757, Republic of Korea.

E-mail address: [dsbyun@hanmail.net](mailto:dsbyun@hanmail.net) (D.-S. Byun).

a sufficient supply of nutrients and the presence of adequate turbulence. In his simple analytical model, Sverdrup's critical depth is a function of average daily light intensity and compensation light intensity. Sverdrup maintained that a net increase in the phytoplankton biomass in the water column occurred in early spring when the depth of the surface mixed layer was less than the "parameterized critical depth". He pointed out that the presence of thermal and/or haline stratification, which affects the thickness of the surface mixed layer, is a "necessary physical condition" for the onset of springtime phytoplankton blooms.

The formation of thermal stratification has been accepted as an essential physical condition for the occurrence of spring phytoplankton blooms in open waters (e.g., Riley, 1957; Nelson and Smith, 1991; Tett and Walne, 1995; Ruardij et al., 1997) and coastal waters (Azumaya et al., 2001). However, as Sverdrup (1953) speculated, spring phytoplankton blooms have also been observed in association with salinity stratification: in South San Francisco Bay by Cloern (1984) and in the Gulf of Maine by Townsend and Spinrad (1986). On the other hand, Townsend et al. (1992) and Eilertsen (1993) observed spring phytoplankton blooms in neutrally-stable clear shelf waters, environments in which physical conditions lead to excessive phytoplankton growth relative to respiration due to the relatively slow vertical excursion rates and deep light penetration. The latter observations have been supported through a simple growth-diffusion model simulation by Huisman et al. (1999). It should be noted that Sverdrup's analytical model lacks the fundamental concept of the "residence time" of phytoplankton in the photic and aphotic zones, a parameter which depends on rates of vertical mixing.

The studies mentioned above imply that vertical mixing is a main controlling factor for the development of spring phytoplankton blooms in open and coastal waters. In open waters (i.e. clear-water environments), seasonal variability (from winter to spring) in the rates and depth of vertical mixing is fundamentally affected by the formation of thermal stratification. Occasionally, spring phytoplankton blooms develop in a neutrally-stable, clear-water column due to clarity and low vertical mixing rates. Unlike in open seas, in tidally-dominated coastal regimes with freshwater inflows the rates of vertical mixing and the depth of the surface mixed layer in spring are influenced by thermal and haline stratification as well as by spring–neap tidal cycles (Legendre, 1981; Cloern, 1991). In tidally-dominated, turbid, coastal environments, vertical mixing rates are also affected by suspended sediment-induced stratification in the bottom boundary layer (Byun and Wang, 2005).

In this paper, we use a 1-D ecosystem model to examine the major controlling physical process for the onset of phytoplankton spring blooms in a tide-

dominated turbid estuarine embayment, the Youngsan River Estuarine Bay (YREB). The YREB is located on the western tip of the southwest coast of Korea (Fig. 1). Tidal characteristics are described as mixed, but predominantly semidiurnal (the tidal form factor, the ratio of diurnal ( $K_1 + O_1$ ) to semidiurnal amplitudes ( $M_2 + S_2$ ), is 0.28) with mean spring and neap tidal ranges of approximately 6 m and 3 m, respectively (Byun et al., 2004; Cho et al., 2004). The YREB is a unique system which functions either as an estuary or as a bay depending on the operation of the water-gates on the Youngsan River Estuary. For most of the time, the YREB operates as a semi-enclosed embayment system, functioning as an estuary only when the water-gates on the Youngsan River Estuary are episodically opened. It should be noted that such freshwater discharge events are usually conducted in less than an hour during low tide conditions.

## 2. Ecosystem model configuration

The 1-D ecosystem model consists of a 1-D biogeochemical model (the European Regional Sea Ecosystem Model, ERSEM) coupled with a 3-D physical model (the Princeton Ocean Model, POM, integrated with a sediment transport model) through the off-line technique (Fig. 2). The 1-D ERSEM, a generic biomass-based biogeochemical model, simulates the biogeochemical dynamics of the coupled pelagic–benthic system. The biological state variables (i.e. carbon (C), nitrogen (N), phosphorus (P) and silicon (Si)) are aggregated into the biological functional groups which comprise trophic levels. The organisms in the model are expressed as vectors of C, N, P, and Si, each of which varies vertically and with time due to hydrodynamics. Three main biological functional groups are identified: the primary producers (phytoplankton), the consumers (zooplankton) and the decomposers (bacteria). The primary physiological processes associated with these organisms (Blackford and Radford, 1995) are: (1) for primary producers, assimilation, respiration, nutrient uptake, exudation, lysis and sedimentation; (2) for consumers, predation, excretion, respiration, mortality and nutrient release; and (3) for decomposers, respiration, nutrient uptake and release, mortality and assimilation of both detritus and dissolved matter. Each of these functional organic groups is further divided according to their morphological and physiological characteristics (e.g., cell size, feeding behavior, growth and respiration rates and uptake preferences), as illustrated in Fig. 3. Net primary productivity in the coupled model is primarily determined by physical and biochemical factors (i.e. solar radiation, nutrients, temperature, turbulence and intracellular nutrient storage). Refer to the following studies for a more detailed description of the biological functional groups: Varela et al. (1995) and Ebenhö

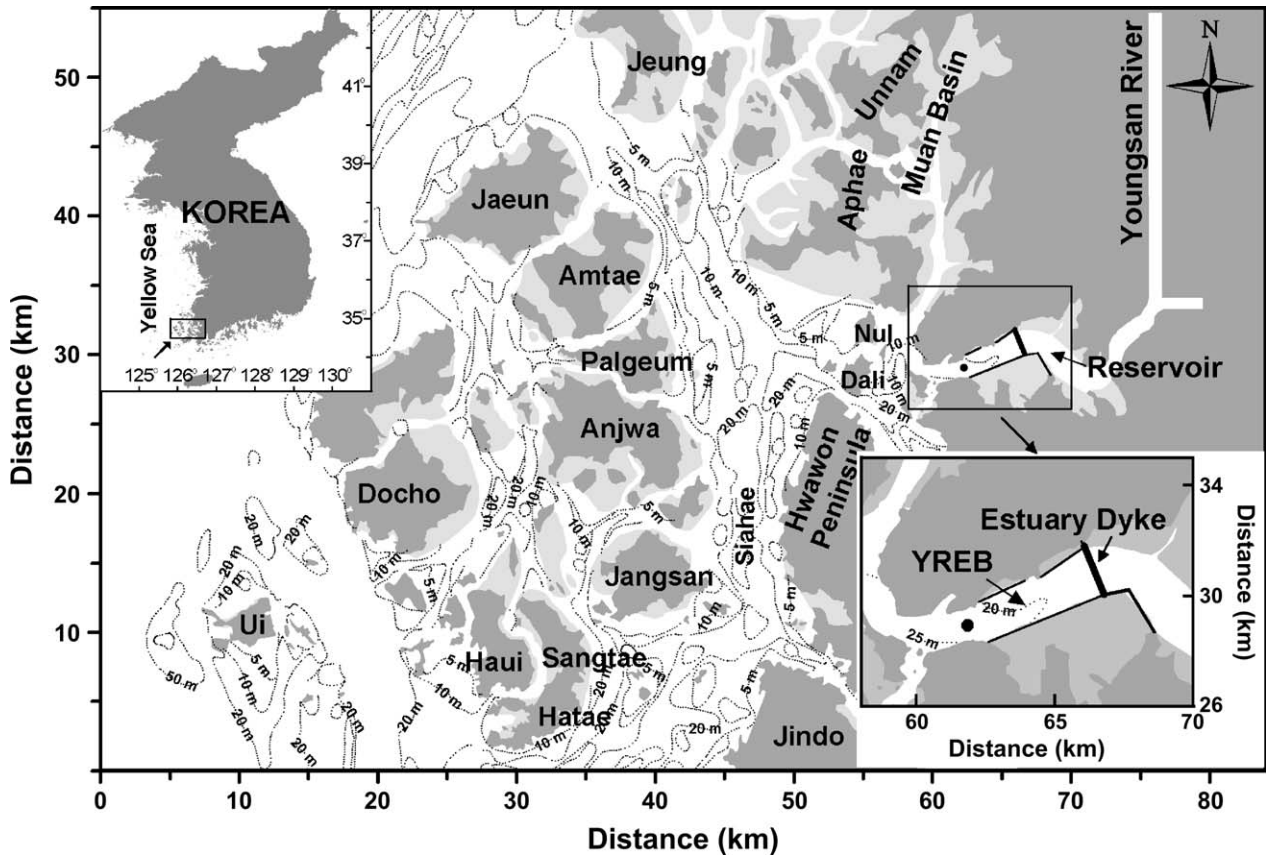


Fig. 1. The physical model domain on the western tip of the southwest coast of Korea. The location of the 1-D ecosystem model is indicated by the circle (●) in the Youngsan River Estuarine Bay (YREB).

et al. (1997) for a description of primary producer modules; Baretta-Bekker et al. (1995) for a description of microzooplankton and bacteria modules; Broekhuizen et al. (1995) for a description of mesozooplankton modules; Baretta-Bekker et al. (1997, 1998) for a description of decoupled carbon assimilation and nutrient uptake, together with intracellular nutrient storage (luxury uptake of nutrients); and Ebenhöf et al. (1995), Ruardij and van Raaphorst (1995) and Blackford (1997)

for a description of the benthic submodel. See Vichi et al. (2003) for a review of the biogeochemical equations used in the ERSEM and Blumberg and Mellor (1987) for a detailed description of the POM.

The 3-D physical model is simulated using the additional forcing factors of surface heat flux (Fig. 4(a)), freshwater discharge (Fig. 4(b)) and wind stress during winter and spring (from January to April) 2001, based on a tide-driven sediment transport model for the western tip of the southwest coast of Korea (Byun and Wang, 2005). This tidal model is forced by the four major constituents ( $M_2$ ,  $S_2$ ,  $K_1$  and  $O_1$ ) and includes the nodal corrections and the astronomical arguments for the 18.61-year Nodal Cycle for the three major lunar constituents (Byun et al., 2004). Its inclusion allows the 3-D physical model to predict the tidal elevation consistent with standard tidal analysis methods. The vertical eddy viscosity and diffusivity are calculated from the Mellor–Yamada level 2.5 turbulence closure scheme (Mellor and Yamada, 1982).

The physical model provides the 1-D ERSEM with the hourly vertical values of diffusivity ( $K_h$ ), temperature ( $T$ ) and salinity ( $S$ ) required to reproduce the physical environment, and the sea level elevation (Ele) and suspended sediment concentration (SSC) values needed

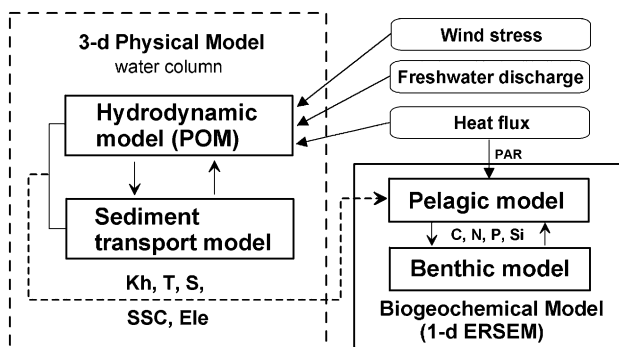


Fig. 2. Schematic diagram of the structure of the 1-D ecosystem model, consisting of a 3-D physical model and a 1-D biogeochemical model coupled through the off-line technique.

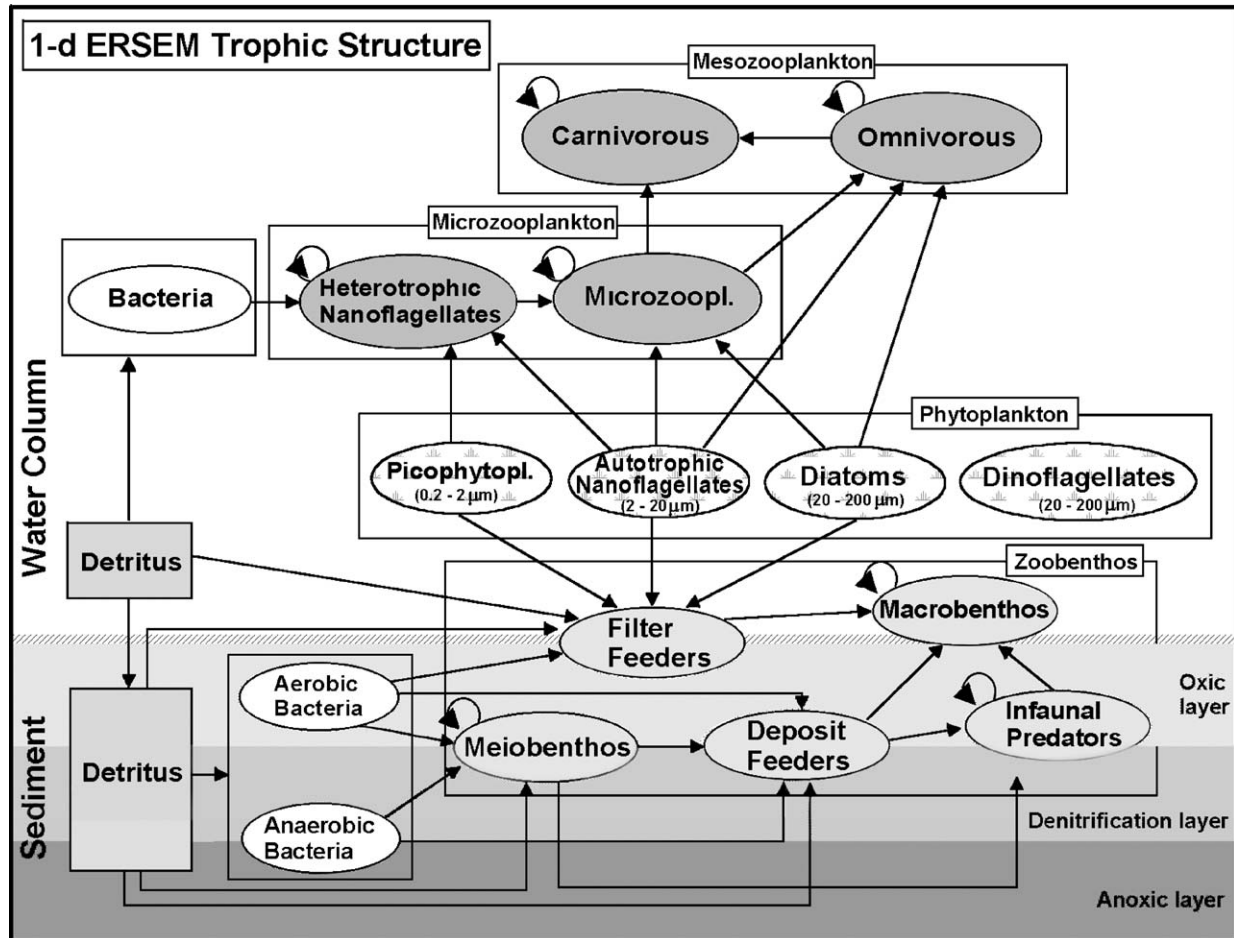


Fig. 3. Schematic diagram of food-web structure in the pelagic and benthic submodels (updated and modified from Allen et al., 1998).

to compute the downward PAR (photosynthetically active radiation) climate in the water column, as shown in Fig. 2. Hourly solar irradiance data, observed at the Mokpo Weather Station near the YREB, were used to calculate the underwater PAR using a conversion factor of 0.46 in the biogeochemical model (Tilzer and Goldman, 1978). It should be noted that the ratio of PAR to total incoming radiation varies from 0.42 to 0.50 for clear-sky conditions, depending on the solar zenith angle, the aerosol thickness and the amount of water vapor (Baker and Frouin, 1987). This ratio is also affected by cloud water droplets due to the predominant selective absorption of near-IR radiation (Siegel et al., 1999), which leads to a conversion factor  $>0.42$ . See Table 1 for monthly variability in each physical parameter used in the ecosystem model.

The inflow of allochthonous nutrients and heat flux by freshwater discharge to the YREB was not considered. Initial values of nutrient and oxygen concentration for the pelagic submodel were obtained from surface and bottom data, averaged over five years of winter (February) measurements taken at the mouth of the YREB between 1997 and 2001 by the National Fisheries

Research and Development Institute of Korea:  $1.36\text{--}2.25\text{ mmol m}^{-3}$  for nitrate,  $0.25\text{--}0.26\text{ mmol m}^{-3}$  for phosphate,  $1.15\text{--}1.20\text{ mmol m}^{-3}$  for ammonia and  $333\text{--}340\text{ mmol m}^{-3}$  for dissolved oxygen. Silicate values ( $6.02\text{--}7.36\text{ mmol m}^{-3}$ ) measured in the surface and bottom waters in winter by Yoon (2001) were also used.

It has been reported that diatoms (specifically, *Thalassiosira* sp. and *Skeletonema costatum*) are the major components of the phytoplankton community in the YREB (Park, 1984; Yoon, 2000). Information on the composition of the phytoplankton groups with respect to cell class and trophic position and their ratios were sourced for the initial condition from Yoon's (2000) study of the YREB: diatoms (75%), autotrophic nanoflagellates (20%) and picophytoplanktons (5%).

The YREB has a depth of 10–25 m and is surrounded by natural barriers in the form of numerous islands. Since dyke construction in 1981 on the Youngsan River Estuary (YRE) and the construction of two seawalls from 1988 to 1994 in the vicinity of the YRE, the maximum tidal current velocities have decreased from  $1\text{ m s}^{-1}$  to  $<0.2\text{ m s}^{-1}$  (Byun et al., 2004). Given these low current velocities, it is assumed that the

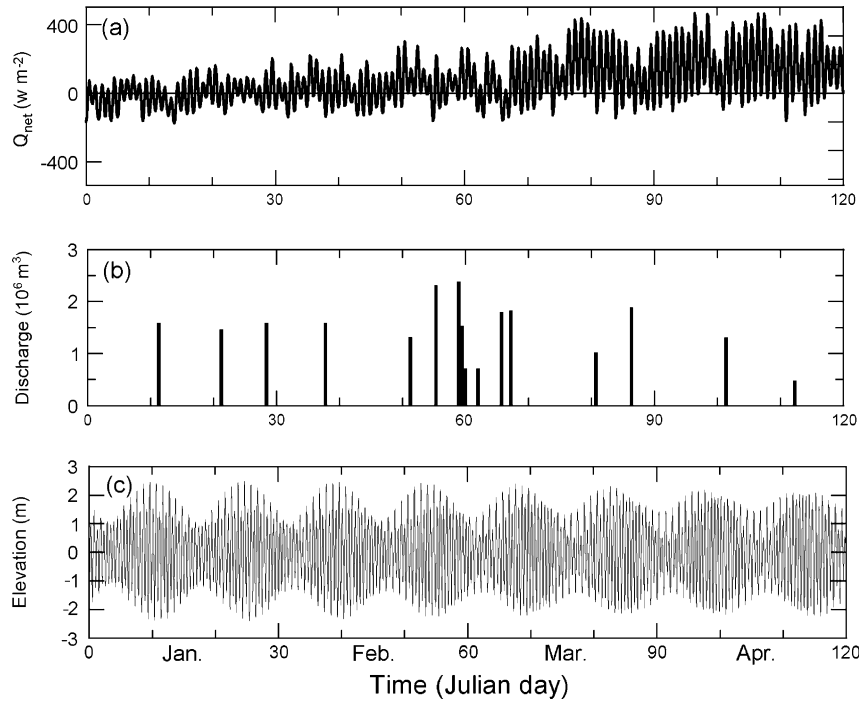


Fig. 4. The time series of daily-filtered net heat flux calculated for the YREB (a), freshwater discharges in the YREB measured by the Korea Agriculture and Rural Infrastructure Corporation (b), and tidal elevations at the YREB station simulated in the physical model from January to April 2001 (c).

horizontal net transport is small enough to be neglected, thus a 1-D ecosystem model can be used to simulate phytoplankton dynamics.

The ecosystem model is applied to a station in the YREB, where observations of chlorophyll-*a* concentration are available and the impacts of direct freshwater discharge forcing are minimal. The model comprises boxes with 18 vertical, sigma ( $\sigma$ ) levels: five logarithmically-distributed layers near the surface ( $\sigma = 0.0, -0.021, -0.042, -0.083$  and  $-0.167$ ) and near the bottom ( $\sigma = -0.917, -0.958, -0.979, -0.990$  and  $-1.000$ ) for the purpose of achieving finer resolution in these

layers, and eight linearly-distributed layers in the middle with an increment of 0.083. It should be noted that the thickness of each box varies with the tides. Sigma levels are given by  $\sigma(k) = (z - \eta) / (\eta + H)$ , where  $k$  ( $= 1, 2, 3, \dots, 17$ ) is the vertical grid index from the surface,  $z$  is the water depth coordinate measured in positive increments from the surface,  $H$  ( $= 21$  m) is the mean water depth and  $\eta$  is the surface elevation which changes with the tides. Thus, the tide-dependent vertical thickness of each box,  $zz(k)$ , is calculated by  $zz(k) = dz(k)(\eta + H)$ , where  $dz(k)$ , the thickness between each sigma level, equals  $\sigma(k + 1) - \sigma(k)$ . See

Table 1  
Monthly mean and standard deviation of key physical environmental parameters simulated or used in the physical model

Parameters	January (1–30 days)	February (31–60 days)	March (61–90 days)	April (91–120 days)
Wind speed ( $\text{m s}^{-1}$ )	$2.6 \pm 1.4$	$2.9 \pm 1.7$	$3.3 \pm 1.7$	$2.4 \pm 1.2$
$T$ ( $^{\circ}\text{C}$ )				
Surface	$6.0 \pm 0.6$	$5.2 \pm 0.4$	$6.3 \pm 1.2$	$10.4 \pm 1.6$
Bottom	$6.4 \pm 0.3$	$5.9 \pm 0.2$	$6.8 \pm 0.7$	$9.4 \pm 0.9$
$S$				
Surface	$31.1 \pm 1.4$	$30.4 \pm 1.9$	$29.6 \pm 2.1$	$31.1 \pm 1.0$
Bottom	$32.0 \pm 0.0$	$31.9 \pm 0.0$	$31.8 \pm 0.1$	$31.9 \pm 0.0$
$K_h$ ( $10^{-3} \text{ m}^2 \text{ s}^{-1}$ )				
Surface	$1.08 \pm 0.8$	$0.81 \pm 0.78$	$0.42 \pm 0.63$	$0.54 \pm 0.81$
Bottom	$0.31 \pm 0.15$	$0.28 \pm 0.10$	$0.28 \pm 0.11$	$0.30 \pm 0.10$
Irradiance ( $\text{W m}^{-2}$ )	$96 \pm 164$	$133 \pm 212$	$187 \pm 268$	$240 \pm 318$
SSC ( $10^{-3} \text{ kg m}^{-3}$ )	$0.45 \pm 0.52$	$0.29 \pm 0.30$	$0.19 \pm 0.25$	$0.12 \pm 0.17$

Mellor (2004) for a more detailed sigma coordinate system.

### 3. Results and discussion

#### 3.1. Thermal and haline stratification

The ecosystem model simulation for the YREB station using the hourly geophysical forcings shows that phytoplankton blooms develop in early March (Fig. 5(a)), a state which is referred to as the “standard run” in this study. The general trend of variability simulated in surface chlorophyll-*a* concentrations is similar to that observed at irregular intervals in the YREB, as shown in Fig. 6. Maximum chlorophyll-*a* concentrations of  $>6 \text{ mg m}^{-3}$  occur during March in the subsurface waters. The major physical processes associated with these blooms, together with the subsurface chlorophyll maxima, are examined below.

Variability in the vertical salinity and temperature structures in the YREB was explored using simulated values derived from the physical model. Fig. 5(b) clearly shows that surface salinity drops in response to freshwater inflow events (see Fig. 4(b)) and variability in the vertical-density structure generally conforms to

that of salinity, as shown in Fig. 5(d). In particular, persistent, strong haline stratification in the surface water column is present between late February and early March as a result of frequent inflows of freshwater from the Youngsan Reservoir into the YREB (day 56–day 68).

In contrast, conspicuous thermal stratification is not shown in early March when phytoplankton blooms develop. Temperature inversions of 1–2 °C are episodically observed in the surface water column from January to March (Fig. 5(c)). A weak thermocline develops in the middle of March due to a gradual increase in the incoming solar radiation and the net heat flux becomes positive, resulting in a heat gain in surface waters as illustrated in Fig. 4(a). In late April, the vertical temperature gradient increases by 2 °C and a relatively strong thermocline develops, leading to thermal stratification of the water column.

It is interesting to note that the episodic occurrence of temperature inversions results from sea-surface cooling events subsequent to haline stratification by freshwater inflows. That is, as water column stability depends predominantly on a strong salinity gradient, heat loss or gain by air–sea interactions is confined to the surface. Similarly, this phenomenon has been observed in the Clyde Sea on the west coast of Scotland (Kasai et al., 1999) and in the tropical Atlantic Ocean associated with

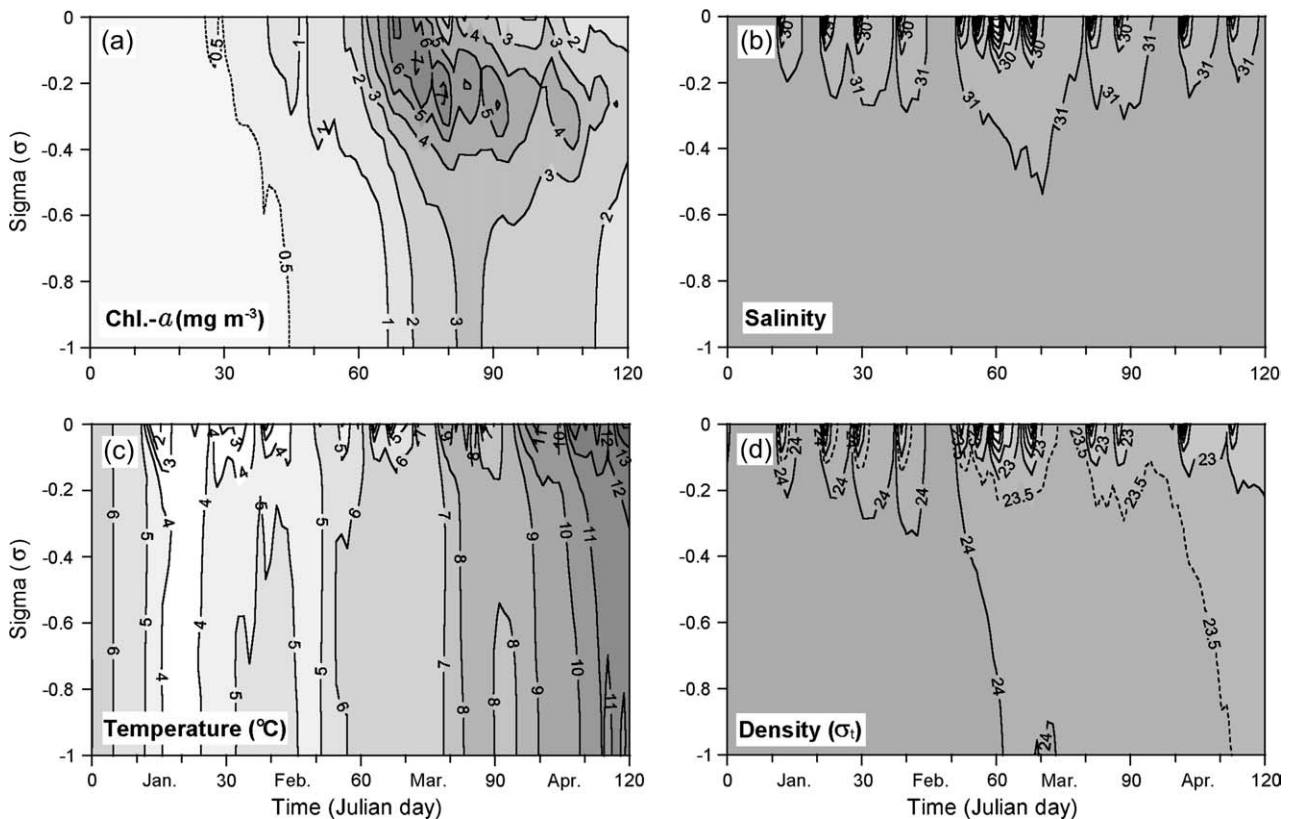


Fig. 5. At the YREB station, variation in the vertical distribution of chlorophyll-*a* concentrations simulated in the ecosystem model (a), and variability in the vertical salinity (b), temperature (c) and density ( $\sigma_t$ ) (d) structures simulated in the physical model.

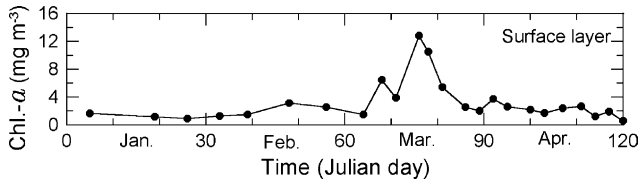


Fig. 6. Variability in chlorophyll-*a* concentration measured 0.5 m below the sea-surface at the YREB station by the Mokpo National University.

Amazon River runoff (Masson and Delecluse, 2001) and is predicted to occur in the northern Adriatic Sea in winter (Wang, 2005).

The vertical eddy diffusivity ( $K_h$ ) simulated by the physical model is examined in order to understand how vertical mixing rates are affected by inputs of buoyant freshwater and sea-surface cooling and warming, tidal

cycles and wind stress. Fig. 7(a, b) shows that the structure and magnitude of vertical mixing in the YREB varied significantly from winter to spring. Furthermore, the bottom  $K_h$  became more-strongly influenced by tidal dynamics, leading to clearer spring–neap cycles.

### 3.2. Vertical mixing rates

In January vertical eddy diffusivity is very high throughout the water column, while in February rates of vertical mixing are gradually reduced (Fig. 7).  $K_h$  decreases vertically to an average of about  $0.53 \times 10^{-3} \text{ m}^2 \text{ s}^{-1}$  in February. High mixing rates occur during winter as a result of sea-surface cooling. This cooling leads to the convective overturn of the water column and, thus, to an increase in turbulent vertical mixing. Additional physical model simulations with and without

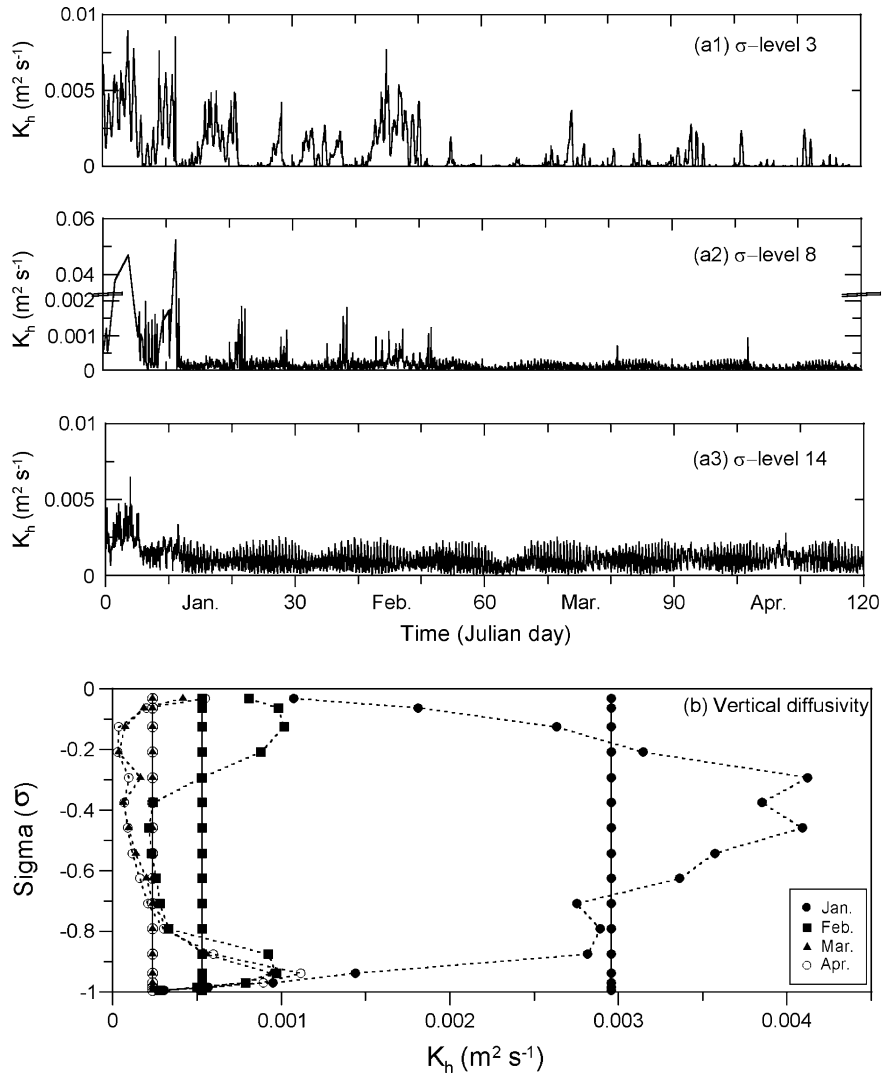


Fig. 7. Variability in the vertical eddy diffusivity ( $K_h$ ) (a) with hourly values for  $\sigma$ -levels 3, 8 and 14 and (b) with monthly-averaged values for each layer (line with dots) and with monthly- and depth-averaged values (straight, solid line) at the YREB station, calculated from the output of the coupled 3-D physical model.

wind stress (not shown) demonstrate that  $K_h$  is little affected by wind stress during winter since there are no strong wind events (see Table 1). As would be predicted according to the findings of Gran and Braarud (1935) and Sverdrup (1953), phytoplankton productivity in the YREB is inhibited during winter mainly because of the active vertical mixing. Low temperatures of approximately 4–6 °C and relatively short day lengths (light availability) are also not suitable physiological conditions for increasing the net growth rate of phytoplankton during winter. However, since the work of Gran (1931), it has commonly been accepted that low temperatures are not a direct limiting factor for phytoplankton growth since phytoplankton blooms are often observed in cold waters: at around 0 °C in the shallow, coastal waters of the North Atlantic by Townsend et al. (1994), at about 3 °C in shelf waters offshore off the Gulf of Maine by Townsend et al. (1992) and at about 6 °C at Malangsdjupet by Eilertsen (1993).

During early March vertical mixing rates are significantly suppressed throughout the entire water column as a result of the frequent buoyant freshwater inputs which occur over a short period during neap tides (Fig. 5(b) and (d)). It can be concluded that the development of phytoplankton blooms in early March primarily results from the dampening of turbulent vertical mixing and stabilization of the water column induced by buoyancy inputs and weak currents, together with an increase in solar radiation. This result is in agreement with the findings of Cloern (1984) and Townsend and Spinrad (1986). The subsurface maximum chlorophyll-*a* concentrations shown in Fig. 5(a) are associated with a surface water nutrient deficiency (mainly silicate) caused by surface diatom blooms, since the supply of nutrients from bottom waters is limited by low vertical mixing rates.

### 3.3. Sensitivity of the $K_h$ parameterization

The model simulation shows that phytoplankton spring blooms can occur in the shallow coastal embayment of the YREB in the absence of thermal stratification, when rates of vertical mixing are markedly reduced by freshwater inflows during neap tidal conditions. Accordingly, the question arises as to how sensitive the development of the phytoplankton spring bloom is to variability in vertical mixing. Further, is it appropriate to use vertically-averaged eddy diffusivity to predict the timing of spring phytoplankton blooms in an ecosystem model?

Two additional numerical experiments were conducted with: (1) monthly-averaged values of  $K_h$  in each layer and (2) monthly depth-averaged values of  $K_h$  (see Fig. 7(b)). That is, in Case 1 there is vertical variation in the monthly-averaged  $K_h$ . In contrast, Case 2 is a model run without vertical variation in the monthly-averaged  $K_h$ . A comparison of these tests and the standard run

reveals the limitations of the parameterization of  $K_h$  in the ecosystem model.

Fig. 8 shows that compared to the standard run, phytoplankton spring blooms are delayed by more than 10 days for Case 1 and 20 days for Case 2. These results indicate that phytoplankton dynamics are very sensitive to rates of vertical mixing and are consistent with the observations of Legendre (1981) and Cloern (1991), which indicate that the period of neap tides is particularly favorable for the development of phytoplankton spring blooms due to their association with relatively-weak vertical mixing rates.

Furthermore, results show that the use of monthly-averaged  $K_h$  values for each model layer and, in particular, depth- and monthly-averaged  $K_h$  values,

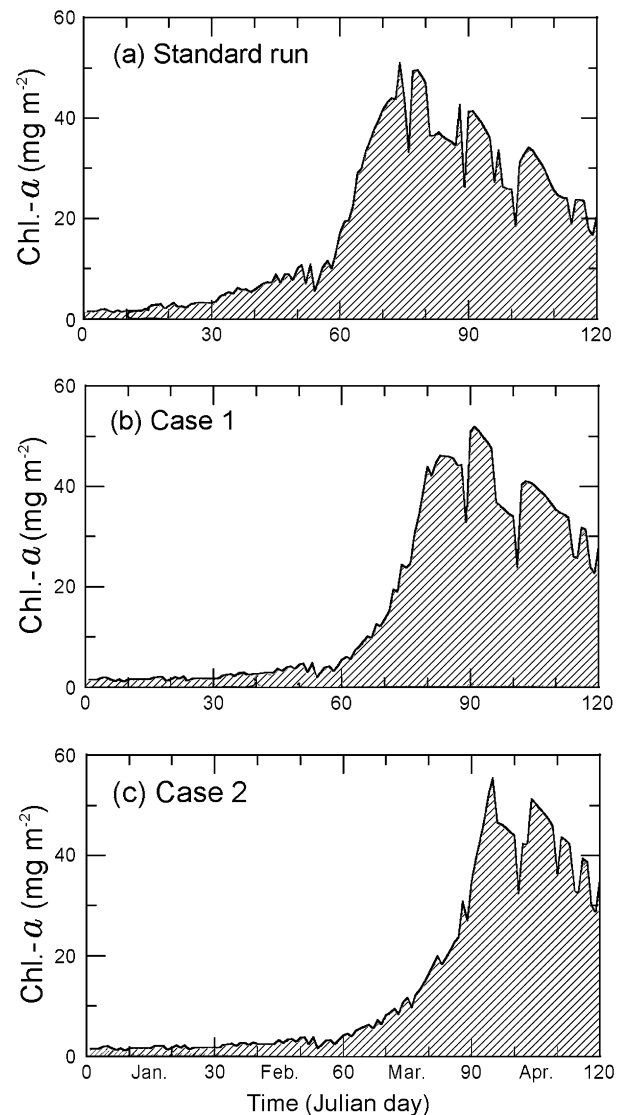


Fig. 8. Daily vertically-integrated chlorophyll-*a* concentrations over the euphotic zone simulated for the YREB station in the ecosystem model for the standard run (a), Case 1 (using monthly-averaged  $K_h$  values for each layer) (b) and Case 2 (using monthly- and depth-averaged  $K_h$  values) (c).

causes the onset of phytoplankton spring blooms to be significantly delayed in the ecosystem model. This delay results because, in comparison to using hourly  $K_h$  values, the use of monthly-averaged  $K_h$  values for each layer leads to the overestimation of vertical mixing in the water column, particularly in the surface mixing layer. The use of monthly, depth-averaged  $K_h$  values leads to an even greater overestimation of vertical mixing, in particular, during neap tides.

#### 4. Conclusions

The onset of phytoplankton blooms in the YREB, a tide-dominated estuarine embayment characterized by weak tidal current velocities, was simulated using a 1-D ecosystem model coupled with a 3-D physical model through the off-line technique. Model results show that the development of phytoplankton spring blooms in the YREB is inhibited by vigorous vertical mixing, particularly during winter when vigorous mixing results from sea-surface cooling processes induced by air–sea interactions, together with the short day length. Model simulations also show that freshwater inflows during neap tides significantly reduce vertical mixing rates and, thus, can trigger phytoplankton spring blooms in shallow estuarine embayments such as the YREB.

Additional model experiments showed that phytoplankton productivity is very sensitive to the use of monthly-averaged vertical eddy diffusivity values ( $K_h$ ) in each model layer and to monthly depth-averaged  $K_h$  values. The resulting overestimation of  $K_h$  leads to significant delays in the development of algal spring blooms, in particular, when depth-averaged values of  $K_h$  are used. These results indicate that the use of vertically-variable, high-frequency  $K_h$  values is preferred in ecosystem models in order to accurately predict the development of phytoplankton blooms.

#### Acknowledgments

The authors would like to acknowledge the kind provision of meteorological data from the Korea Meteorological Administration and freshwater discharge data from the Korea Agriculture and Rural Infrastructure Corporation. We thank Professor Kyung-Yang Park of the Mokpo National University for providing chlorophyll-*a* concentration data. The numerical model simulations were conducted using the AlphaServer SC system of the Australian Partnership for Advanced Computing (APAC) National Facility. The authors wish to thank Dr. Marco Zavatarelli and two anonymous reviewers for constructive comments, which helped to significantly improve this work. This work was supported by grant No. RO1-2004-000-10771-0

from the Basic Research Program of the Korea Science & Engineering Foundation.

#### References

- Allen, J.I., Blackford, J.C., Radford, P.J., 1998. A 1-D vertically resolved modelling study of the ecosystem dynamics of the middle and southern Adriatic Sea. *Journal of Marine System* 18, 265–286.
- Azumaya, T., Isoda, Y., Noriki, S., 2001. Modeling of the spring bloom in Funka Bay, Japan. *Continental Shelf Research* 21, 473–494.
- Baker, K.S., Frouin, R., 1987. Relation between photosynthetically available radiation and total insolation at the Ocean Surface Under Clear Skies. *Limnology and Oceanography* 32, 1370–1377.
- Baretta-Bekker, J.G., Baretta, J.W., Rasmussen, E.K., 1995. The microbial food web in the European Regional Seas Ecosystem Model. *Netherlands Journal of Sea Research* 33, 363–379.
- Baretta-Bekker, J.G., Baretta, J.W., Ebenhö, W., 1997. Microbial dynamics in the marine ecosystem model ERSEM II with decoupled carbon assimilation and nutrient uptake. *Journal of Sea Research* 38, 195–211.
- Baretta-Bekker, J.G., Baretta, J.W., Hansen, A.S., Riemann, B., 1998. An improved model of carbon and nutrient dynamics in the microbial food web in marine enclosures. *Aquatic Microbial Ecology* 14, 91–108.
- Blackford, J.C., 1997. An analysis of benthic biological dynamics in a North Sea ecosystem model. *Journal of Sea Research* 38, 213–230.
- Blackford, J.C., Radford, P.J., 1995. A structure and methodology for marine ecosystem modelling. *Netherlands Journal of Sea Research* 33, 247–260.
- Blumberg, A.F., Mellor, G.L., 1987. A description of a three-dimensional coastal ocean circulation model. In: Nihoul, J.C.J., Jamart, B.M. (Eds.), *Three-Dimensional Models of Marine and Estuarine Dynamics*, Elsevier Oceanography Series, vol. 45. Elsevier, New York, pp. 55–88.
- Broekhuizen, N., Heath, M.R., Hay, S.J., Gurney, W.S.C., 1995. Modelling the dynamics of the North Sea's mesozooplankton. *Netherlands Journal of Sea Research* 33, 381–406.
- Byun, D.S., Wang, X.H., Holloway, P.E., 2004. Tidal characteristic adjustment due to dyke and seawall construction in the Mokpo Coastal Zone, Korea. *Estuarine, Coastal and Shelf Science* 59, 185–196.
- Byun, D.S., Wang, X.H., 2005. The effect of sediment stratification on tidal dynamics and sediment transport patterns. *Journal of Geophysical Research* 110 (C03011), doi:10.1029/2004JC002459.
- Cho, Y.K., Park, L.H., Cho, C., Lee, I.T., Park, K.Y., Oh, C.W., 2004. Multi-layer structure in the Youngsan Estuary, Korea. *Estuarine, Coastal and Shelf Science* 61, 325–329.
- Cloern, J.E., 1984. Temporal dynamics and ecological significance of salinity stratification in an estuary (South San Francisco Bay, USA). *Oceanologica Acta* 7, 137–140.
- Cloern, J.E., 1991. Tidal stirring and phytoplankton bloom dynamics in an estuary. *Journal of Marine Research* 49, 203–221.
- Ebenhö, W., Baretta-Bekker, J.G., Baretta, J.W., 1997. The primary production module in the marine ecosystem model ERSEM II, with emphasis on the light forcing. *Journal of Sea Research* 38, 173–193.
- Ebenhö, W., Kohlmeier, C., Radford, P.J., 1995. The benthic biological submodel in the European Seas Ecosystem Model. *Netherlands Journal of Sea Research* 33, 423–452.
- Eilertsen, H.C., 1993. Spring blooms and stratification. *Nature* 363, 24.
- Gran, H.H., 1931. On the conditions for the production of plankton in the sea. *Rapports et Process-Verbaux des Reunions – Conseil International Pour l'Exploration de la Mer* 75, 37–46.
- Gran, H.H., Braarud, T., 1935. A quantitative study of the phytoplankton in the Bay of Fundy and the Gulf of Maine. *Journal of the Biological Board of Canada* 1, 279–467.

- Huisman, J., Von Oostveen, P., Weissing, F.J., 1999. Critical depth and critical turbulence: two different mechanisms for the development of phytoplankton blooms. *Limnology and Oceanography* 44, 1781–1787.
- Kasai, A., Rippeth, T.P., Simpson, J.H., 1999. Density and flow structure in the Clyde Sea front. *Continental Shelf Research* 19, 1833–1848.
- Legendre, L., 1981. Hydrodynamic control of marine phytoplankton production: the paradox of stability. In: Nihoul, J.C.J. (Ed.), *Ecohydrodynamics*. Oceanography Series 32. Elsevier Press, Amsterdam, pp. 191–207.
- Masson, S., Delecluse, P., 2001. Influence of the Amazon River Runoff on the Tropical Atlantic. *Physics and Chemistry of the Earth* 26, 137–142.
- Mellor, G.L., Yamada, T., 1982. Development of a turbulence closure model for geophysical fluid problems. *Reviews of Geophysics and Space Physics* 20, 851–875.
- Mellor, G.L., 2004. Users Guide for a Three-Dimensional, Primitive Equation, Numerical Ocean Model. In: Report: Program in Atmospheric and Oceanic Sciences, Princeton University, Princeton, NJ 08544-0710, 56 pp.
- Nelson, D.M., Smith, W.O., 1991. Sverdrup revisited: critical depths, maximum chlorophyll levels, and the control of Southern Ocean productivity by the irradiance-mixing regime. *Limnology and Oceanography* 36, 1650–1661.
- Park, K.Y., 1984. On the phytoplankton of the Mokpo bay in spring. *Bulletin of Institute of Littoral Biota, Mokpo National University* 1, 57–65 (in Korean).
- Riley, G.A., 1957. Phytoplankton of the North Central Sargasso Sea, 1950–52. *Limnology and Oceanography* 35, 228–234.
- Ruardij, P., van Raaphorst, W., 1995. Benthic nutrient regeneration in the ERSEM ecosystem model of the North Sea. *Netherlands Journal of Sea Research* 33, 453–483.
- Ruardij, P., van Haren, H., Ridderinkhof, H., 1997. The impact of thermal stratification on phytoplankton and nutrient dynamics in shelf seas: a model study. *Journal of Sea Research* 38, 311–331.
- Siegel, D.A., Westberry, T.K., Ohlmann, J.C., 1999. Cloud color and ocean radiant heating. *Journal of Climate* 12, 1101–1116.
- Smetacek, V., Passow, U., 1990. Spring bloom initiation and Sverdrup's critical-depth model. *Limnology and Oceanography* 35, 228–234.
- Sverdrup, H.U., 1953. On conditions for vernal blooming of phytoplankton. *Journal du Conseil – Conseil International Pour l'Exploration de la Mer* 18, 287–295.
- Tett, P., Walne, A., 1995. Observations and simulations of hydrography, nutrients and plankton in the southern North Sea. *Ophelia* 42, 371–416.
- Tilzer, M.M., Goldman, C.R., 1978. Importance of mixing, thermal stratification and light adaptation for phytoplankton productivity in Lake Tahoe (California–Nevada). *Ecology* 59, 810–821.
- Townsend, D.W., Keller, M.D., Sieracki, M.E., Ackleson, S.G., 1992. Spring phytoplankton blooms in the absence of vertical water column stratification. *Nature* 360, 59–62.
- Townsend, D.W., Cammen, L.M., Holligan, P.M., Campbell, D.E., Pettigrew, N.R., 1994. Causes and consequences of variability in the timing of spring phytoplankton blooms. *Deep Sea Research Part I* 41, 747–765.
- Townsend, D.W., Spinrad, R.W., 1986. Early spring phytoplankton blooms in the Gulf of Maine. *Continental Shelf Research* 6, 515–529.
- Varela, R.A., Cruzado, A., Gabaldón, J.E., 1995. Modelling primary production in the North Sea using the European Regional Seas Ecosystem Model. *Netherlands Journal of Sea Research* 33, 337–361.
- Vichi, M., Baretta, J.W., Baretta-Bekker, J.G., Ebenhöf, W., Kohlmeier, C., Ruardij, P., 2003. European Regional Seas Ecosystem Model. III: Review of the Biogeochemical Equations, 88 pp.
- Wang, X.H., 2005. Circulation and heat budget of the northern Adriatic Sea (Italy) due to a Bora event in January 2001: a numerical model study. *Ocean Modelling* 10, 253–271.
- Yoon, Y.H., 2000. On the distributional characteristics of phytoplankton community in Mokpo Coastal Waters, Southwestern Korea during low temperature season. *Journal of Institute for Basic Sciences, Yosu Nat'l Univ.* 2, 71–82 (in Korean).
- Yoon, Y.H., 2001. On the spatio-temporal distributions of water quality and chlorophyll *a*, and the environmental factors on the variation of the phytoplankton biomass in the Mokpo Coastal Waters, Southwestern Korea during low temperature season. *Journal of Korean Society on Water Quality* 17 (1), 1–13 (in Korean).